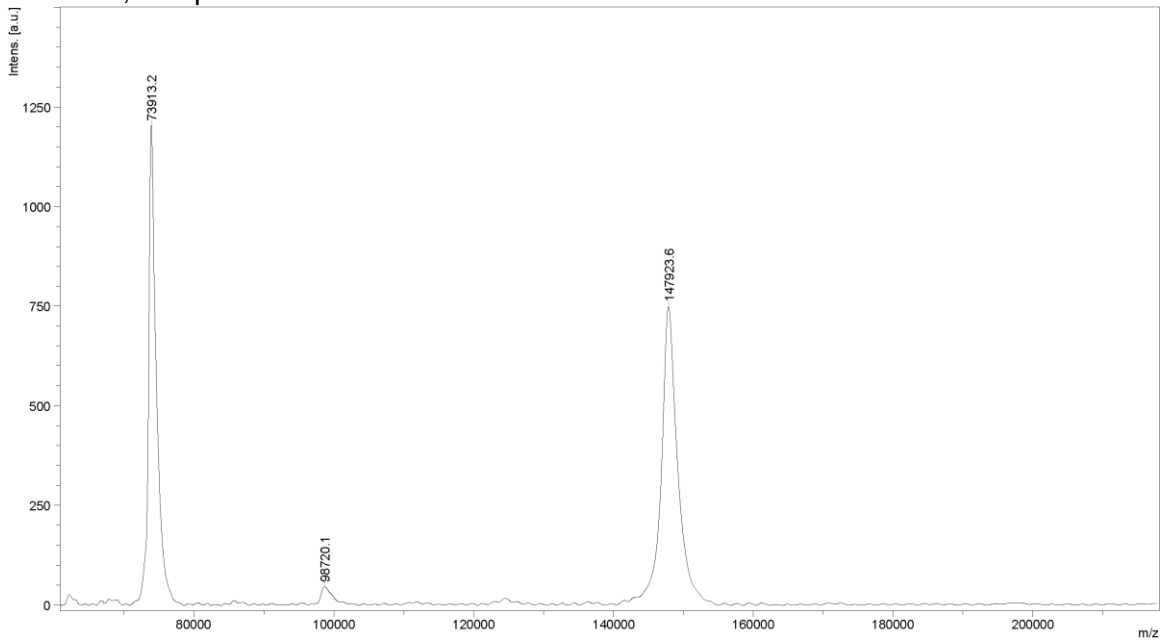
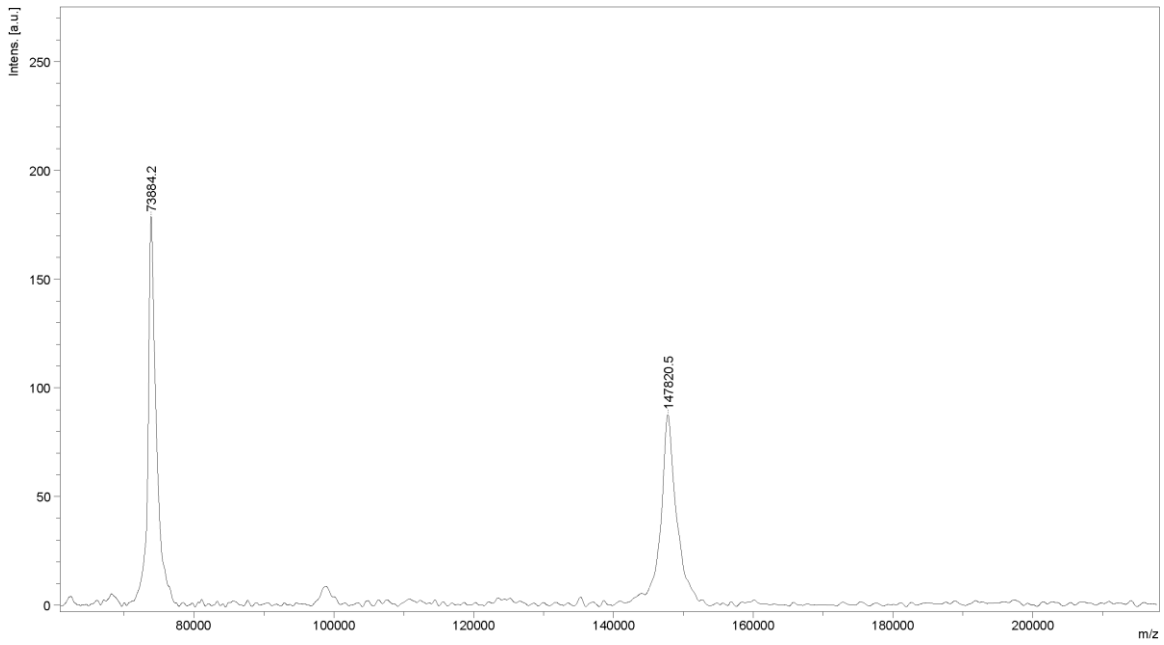


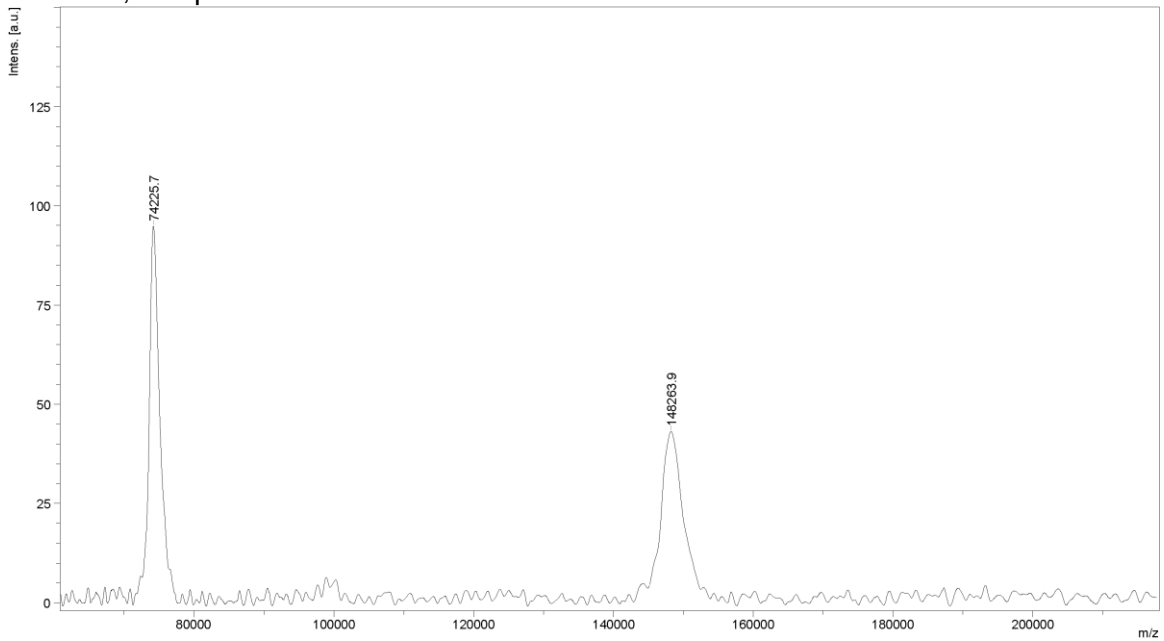
**Supplemental Fig. 1.** MALDI-TOF MS/MS mass spectrometry analysis of unmodified AMG102, sample #1.



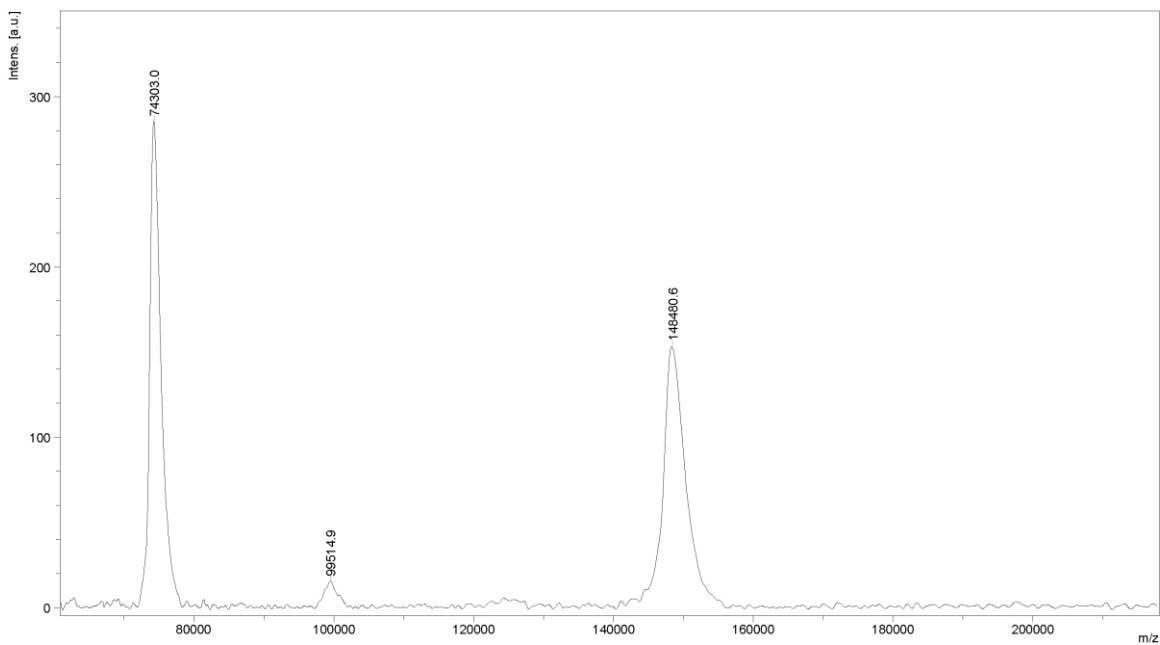
**Supplemental Fig. 2.** MALDI-TOF MS/MS mass spectrometry analysis of unmodified AMG102, sample #2.



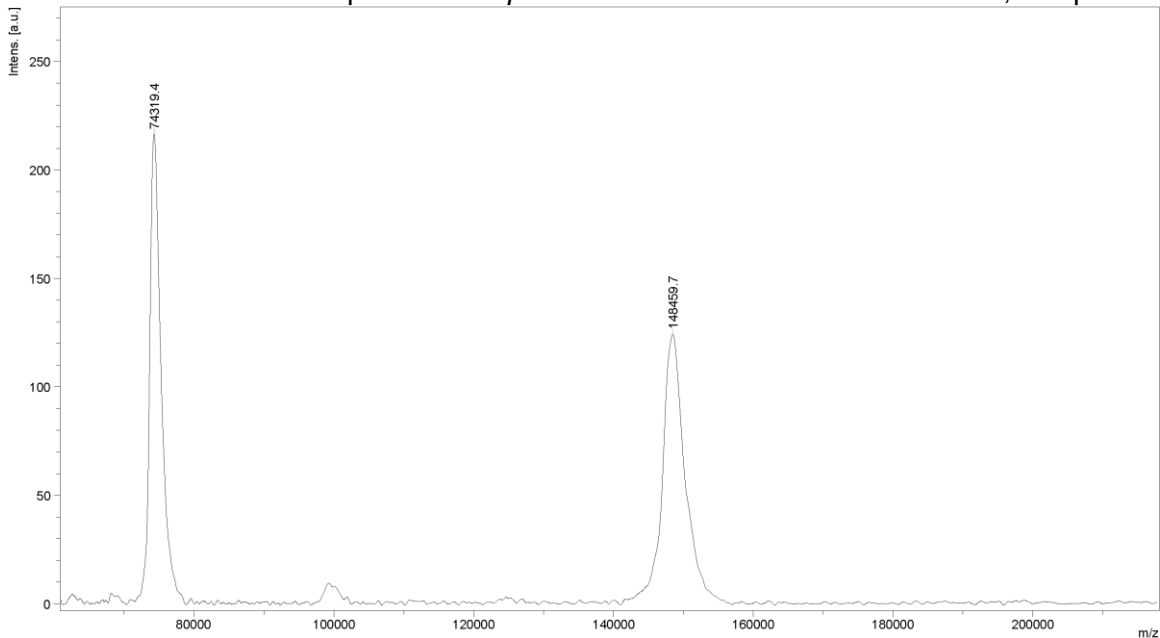
**Supplemental Fig. 3.** MALDI-TOF MS/MS mass spectrometry analysis of unmodified AMG102, sample #3.



**Supplemental Fig. 4.** MALDI-TOF MS/MS mass spectrometry analysis of AMG102 that had been reacted with 5 equivalents of *p*-SCN-Bn-DFO to form DFO-AMG102, sample #1.



**Supplemental Fig. 5.** MALDI-TOF MS/MS mass spectrometry analysis of AMG102 that had been reacted with 5 equivalents of *p*-SCN-Bn-DFO to form DFO-AMG102, sample #2.



**Supplemental Fig. 6.** MALDI-TOF MS/MS mass spectrometry analysis of AMG102 that had been reacted with 5 equivalents of *p*-SCN-Bn-DFO to form DFO-AMG102, sample #3.

**Supplemental Table 1.** MALDI-TOF MS/MS results of AMG102 and AMG102-DFO, submitted as 1 µg/µL solutions, 10 µL total, analyzed by the University of Alberta Mass Spectrometry Facility, with mass units as daltons (Da).

	AMG102 standard		AMG102 DFO	
	(m+2/2)	Full mass	(m+2/2)	Full mass
Mass (Da)	73900.8	147801.6	74225.7	148451.4
Mass (Da)	73913.2	147826.4	74303.0	148606.0
Mass (Da)	73884.2	147768.4	74319.4	148638.8
Average Mass (Da)	73899.4	147798.8	74282.7	148565.4
Std. Dev (Da)	14.6	29.1	50.0	100.1

Immunoconjugate	Mass difference (Da)	Chelate mass (Da)	Chelates/antibody average	Standard Deviation
AMG102-DFO	766.6	752.9	1.0	0.1

**Supplemental Table 2.** Biodistribution data of <sup>89</sup>Zr-DFO-AMG102 or <sup>89</sup>Zr-DFO-IgG (as indicated in table) (~20-30 µCi, 0.74-1.1 MBq, ~5 µg, in 200-250 µL of sterile saline; tumor volume ~ 100-150 mm<sup>3</sup>) in female nude athymic mice bearing subcutaneous xenografts of U87MG or MKN45 (as indicated in table).

<sup>89</sup> Zr-DFO-antibody	AMG102			AMG102			AMG102		
	U87MG			U87MG			U87MG		
Biodistribution time	24 h			48 h			72 h		
Organ	%ID/g	Std. Dev.	n	%ID/g	Std. Dev.	n	%ID/g	Std. Dev.	n
Blood	23.3	1.2	5	22.8	1.9	5	20.5	2.1	5
Tumor	19.1	3.2	5	30.2	5.9	5	40.3	3.9	5
Heart	6.6	0.9	5	5.3	0.1	5	5.4	0.5	5
Lungs	9.3	2.0	5	10.4	1.4	5	11.2	1.5	5
Liver	6.1	1.0	5	5.7	1.1	5	6.7	0.3	5
Spleen	4.1	0.1	5	5.0	0.5	5	5.9	0.5	5
Pancreas	2.1	0.3	5	2.1	0.4	5	2.0	0.2	5
Stomach	1.6	0.4	5	1.7	0.6	5	1.2	0.5	5
Small Intestine	2.1	0.2	5	2.4	0.5	5	2.1	0.3	5
Large Intestine	1.2	0.3	5	1.3	0.3	5	1.0	0.2	5
Kidney	6.1	0.6	5	6.8	0.7	5	6.0	0.8	5
Muscle	1.8	0.2	5	1.5	0.2	5	1.4	0.2	5
Bone	4.4	0.3	5	4.4	0.7	5	6.8	0.9	5
Skin	6.9	1.4	5	5.0	0.6	5	7.7	0.3	5

**Supplemental Table 3.** Biodistribution data of <sup>89</sup>Zr-DFO-AMG102 or <sup>89</sup>Zr-DFO-IgG (as indicated in table) (~20-30 µCi, 0.74-1.1 MBq, ~5 µg, in 200-250 µL of sterile saline; tumor volume ~ 100-150 mm<sup>3</sup>) in female nude athymic mice bearing subcutaneous xenografts of U87MG or MKN45 (as indicated in table).

<sup>89</sup> Zr-DFO-antibody	AMG102			AMG102 + blocking (500 µg AMG102)			Human IgG			AMG102		
	U87MG			U87MG			U87MG			MKN45		
Biodistribution time	120 h			120 h			120 h			120 h		
Organ	%ID/g	Std. Dev.	n	%ID/g	Std. Dev.	n	%ID/g	Std. Dev.	n	%ID/g	Std. Dev.	n
Blood	15.2	2.0	5	19.4	1.4	5	9.9	4.3	5	10.6	1.9	10
Tumor	36.8	7.8	5	29.7	8.6	5	11.5	3.3	5	5.0	1.3	10
Heart	4.9	0.1	5	6.4	0.8	5	3.7	1.1	5	2.7	0.5	10
Lungs	8.3	1.8	5	10.4	1.6	5	5.7	1.8	5	5.9	1.0	10
Liver	5.6	0.5	5	5.8	0.4	5	12.1	1.8	5	5.3	1.2	10
Spleen	5.3	0.8	5	5.7	0.9	5	7.2	1.3	5	3.5	0.6	10
Pancreas	1.9	0.3	5	2.0	0.3	5	1.3	0.3	5	1.0	0.2	10
Stomach	1.4	0.2	5	1.7	0.4	5	1.2	0.2	5	0.8	0.3	10
Small Intestine	1.4	0.1	5	1.7	0.1	5	1.3	0.2	5	0.9	0.2	10
Large Intestine	0.8	0.1	5	0.8	0.1	5	0.6	0.1	5	0.7	0.2	10
Kidney	5.0	0.5	5	5.8	1.3	5	5.2	0.8	5	3.7	0.5	10
Muscle	1.3	0.2	5	1.5	0.3	5	0.9	0.2	5	0.7	0.1	10
Bone	6.2	1.0	5	7.0	2.4	5	10.0	2.4	5	2.1	0.3	10
Skin	5.4	1.2	5	5.9	0.5	5	4.4	0.3	5	4.8	1.1	10

**Supplemental Table 4.** Biodistribution data displayed as %ID of <sup>89</sup>Zr-DFO-AMG102 (~20-30 µCi, 0.74-1.1 MBq, ~5 µg, in 200-250 µL of sterile saline; tumor volume ~ 100-150 mm<sup>3</sup>) in female nude athymic mice bearing subcutaneous xenografts of U87MG, with data displayed as %ID to properly highlight blocking efficacy, due to dramatic tumor shrinkage observed in the blocking group.

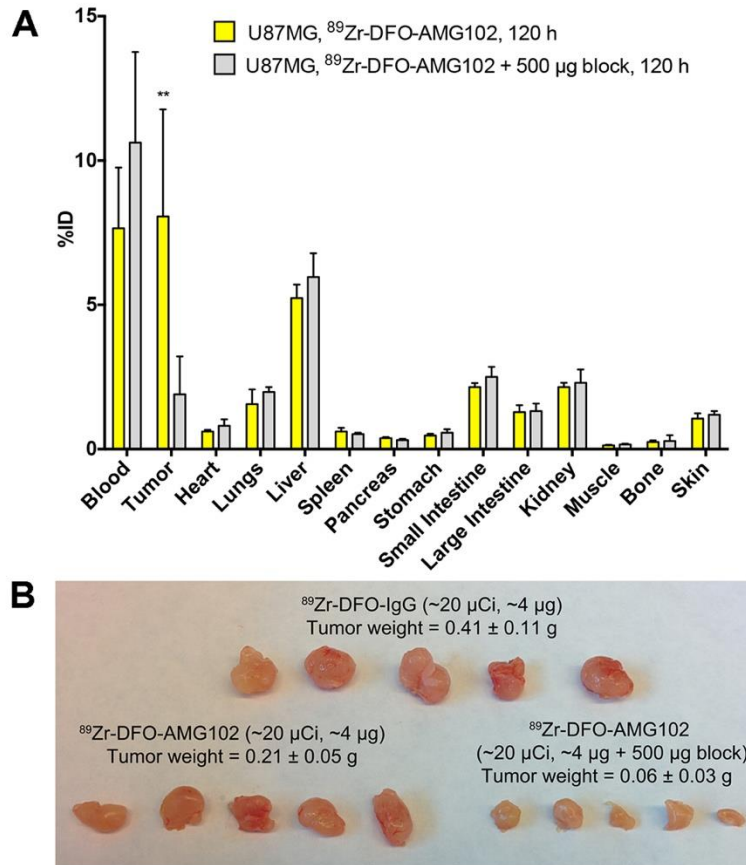
Organ	U87MG, <sup>89</sup> Zr-DFO-AMG102, 120 h			U87MG, <sup>89</sup> Zr-DFO-AMG102, 500 µg block, 120 h		
	%ID	Std. Dev.	n	%ID	Std. Dev.	n
Blood	7.7	2.1	5	10.6	3.1	5
Tumor	8.1	3.7	5	1.9	1.3	5
Heart	0.6	0.1	5	0.8	0.2	5
Lungs	1.6	0.5	5	2.0	0.2	5
Liver	5.2	0.5	5	6.0	0.8	5
Spleen	0.6	0.1	5	0.5	0.1	5
Pancreas	0.4	0.04	5	0.3	0.1	5
Stomach	0.5	0.1	5	0.6	0.1	5
Small Intestine	2.2	0.1	5	2.5	0.4	5
Large Intestine	1.3	0.2	5	1.3	0.3	5
Kidney	2.2	0.2	5	2.3	0.5	5
Muscle	0.1	0.02	5	0.2	0.03	5
Bone	0.3	0.1	5	0.3	0.2	5
Skin	1.1	0.2	5	1.2	0.1	5

**Supplemental Table 5.** Biodistribution data shown as tumor/organ ratios of <sup>89</sup>Zr-DFO-AMG102 or <sup>89</sup>Zr-DFO-IgG (as indicated in table) (~20-30 μCi, 0.74-1.1 MBq, ~5 μg, in 200-250 μL of sterile saline; tumor volume ~ 100-150 mm<sup>3</sup>) in female nude athymic mice bearing subcutaneous xenografts of U87MG or MKN45.

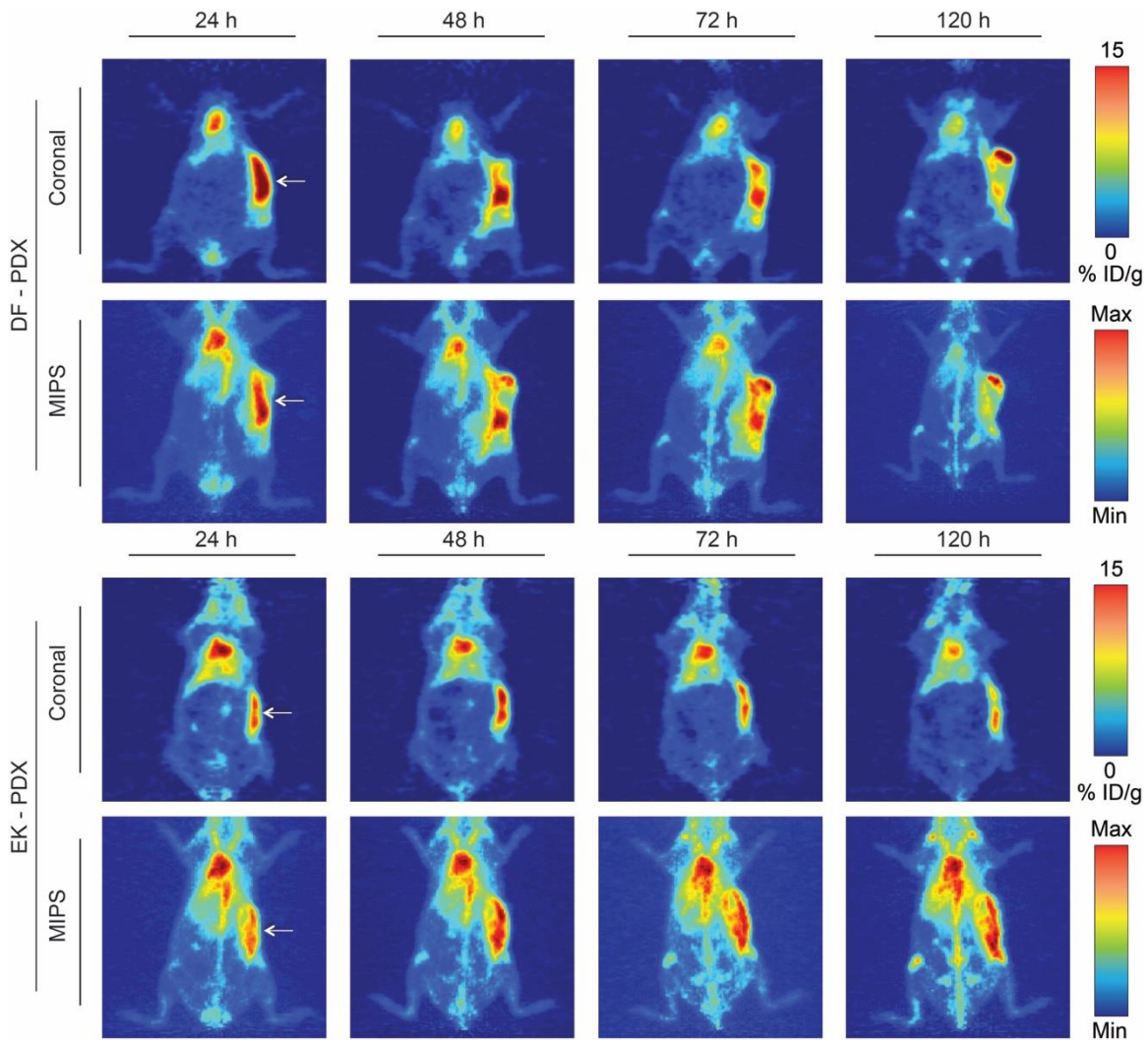
<sup>89</sup> Zr-DFO-antibody	AMG102						
	AMG102	AMG102	AMG102	AMG102	block	human IgG	AMG102
Tumor xenograft	U87MG	U87MG	U87MG	U87MG	U87MG	U87MG	MKN45
Biodistribution time	24 h	48 h	72 h	120 h	120 h	120 h	120 h
Tumor / Blood ratio	0.8	1.3	2.0	2.4	1.5	1.2	0.4
Tumor / Heart ratio	2.9	5.7	7.5	7.5	4.6	3.1	1.7
Tumor / Lungs ratio	2.1	2.9	3.6	4.4	2.9	2.0	0.9
Tumor / Liver ratio	3.1	5.3	6.0	6.6	5.1	1.0	1.0
Tumor / Kidney ratio	3.1	4.4	6.8	7.3	5.1	2.2	1.4
Tumor / Bone ratio	4.4	6.9	5.9	6.0	4.3	1.2	2.5
Tumor / organ Std. Dev.	24 h	48 h	72 h	120 h	120 h	120 h	120 h
Tumor / Blood ratio	0.1	0.3	0.3	0.6	0.5	0.6	0.1
Tumor / Heart ratio	0.6	1.1	1.0	1.6	1.5	1.3	0.5
Tumor / Lungs ratio	0.6	0.7	0.6	1.4	0.9	0.9	0.3
Tumor / Liver ratio	0.7	1.4	0.6	1.5	1.5	0.3	0.4
Tumor / Kidney ratio	0.6	1.0	1.1	1.7	1.9	0.7	0.4
Tumor / Bone ratio	0.8	1.7	0.9	1.6	1.9	0.4	0.7

**Supplemental Table 6.** Biodistribution data of <sup>89</sup>Zr-DFO-AMG102 (~20-30 μCi, 0.74-1.1 MBq, ~5 μg, in 200-250 μL of sterile saline) post PET imaging at 120 h p.i. in patient-derived xenograft models (PDX) in female nude athymic mice bearing.

Tumor xenograft	PDX-DY			PDX-DC			PDX-DF			PDX-EK		
	%ID/g	Std. Dev.	n	%ID/g	Std. Dev.	n	%ID/g	Std. Dev.	n	%ID/g	Std. Dev.	n
Blood	15.1		1	13.4		1	11.6	4.6	2	13.4	2.3	3
Tumor	4.5	0.02	2	4.5	1.6	2	6.6	0.2	2	6.8	0.4	3
Heart	4.0		1	3.0		1	2.7	0.8	2	3.3	0.4	3
Lungs	9.3		1	7.7		1	6.2	3.2	2	5.8	1.4	3
Liver	5.3		1	4.6		1	4.7	0.3	2	6.4	0.7	3
Spleen	12.1		1	11.4		1	8.1	2.2	2	11.8	1.6	3
Pancreas	1.4		1	1.3		1	1.1	0.5	2	1.1	0.1	3
Stomach	1.5		1	1.1		1	1.0	0.03	2	0.8	0.2	3
Small Intestine	1.6		1	1.5		1	1.1	0.3	2	1.3	0.1	3
Large Intestine	1.1		1	1.0		1	0.8	0.1	2	0.9	0.1	3
Kidney	4.6		1	4.6		1	3.7	1.7	2	4.0	0.5	3
Muscle	1.2		1	1.2		1	0.8	0.3	2	0.7	0.1	3
Bone	5.6		1	4.0		1	4.7	2.6	2	3.9	0.5	3
Skin	5.4		1	4.8		1	3.4	1.1	2	5.8	1.4	3

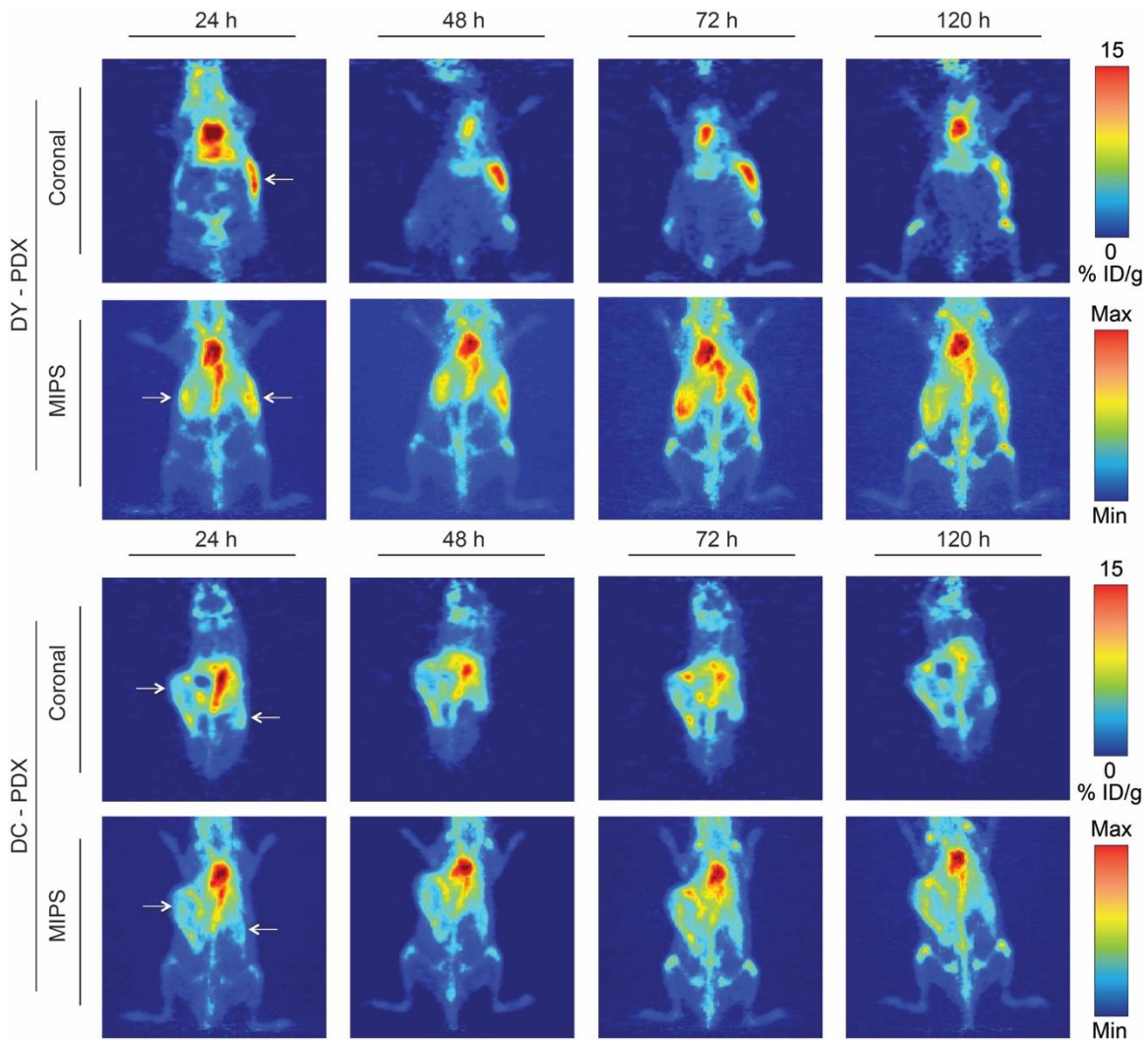


**Supplemental Fig. 7.** (A) a comparison of blocking and non-blocking groups from the biodistribution data of <sup>89</sup>Zr-DFO-AMG102 at 120 with data expressed as %ID, showing similar %ID values for all tissues except for statistically significantly less uptake in blocked tumors; and (B) a photograph of tumors from these biodistribution experiments showing the difference in size between groups. Data in Supplemental Tables 2-5, statistical significance shown from students unpaired t-test using PRISM software, \* = ≤ 0.05 \*\* = ≤ 0.01 \*\*\* = ≤ 0.001.

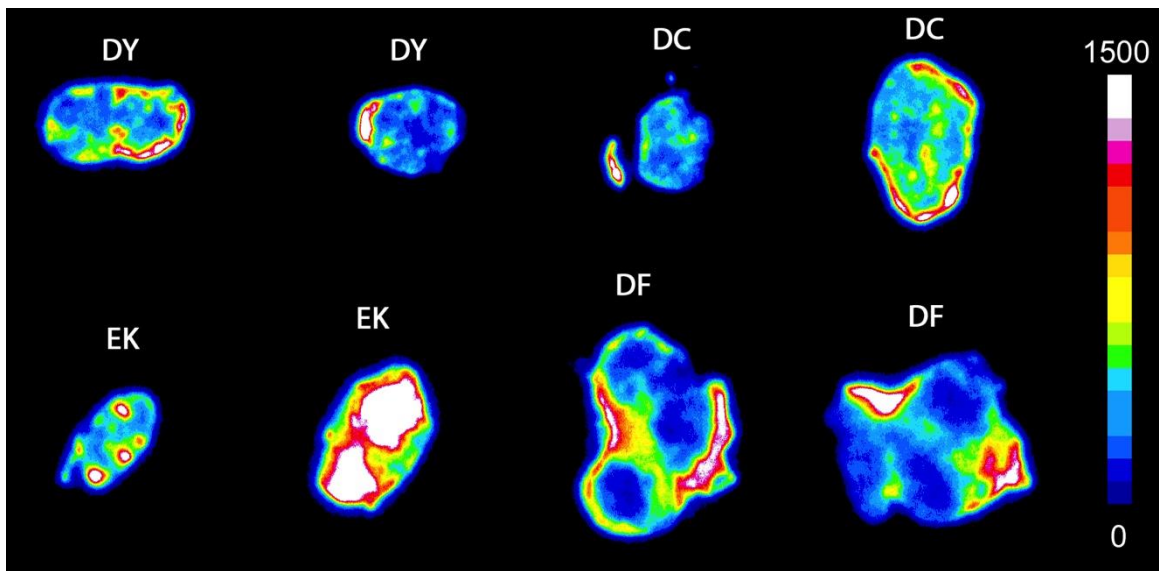


**Supplemental Fig. 8.** Serial PET imaging of  $^{89}\text{Zr}$ -DFO-AMG102 in PDX DF and EK bearing mice with unknown levels of HGF at 24, 48, 72, and 120 h p.i. ( $\sim 30 \mu\text{g}$ ,  $\sim 130\text{-}150 \mu\text{Ci}$ ,  $\sim 4.8\text{-}5.6 \text{ MBq}$ ,  $200 \mu\text{L}$  sterile saline), showing low uptake in tumors suggesting very low levels of HGF protein,  $\sim 5\text{-}10 \text{ \%ID/g}$ , EPR uptake only.

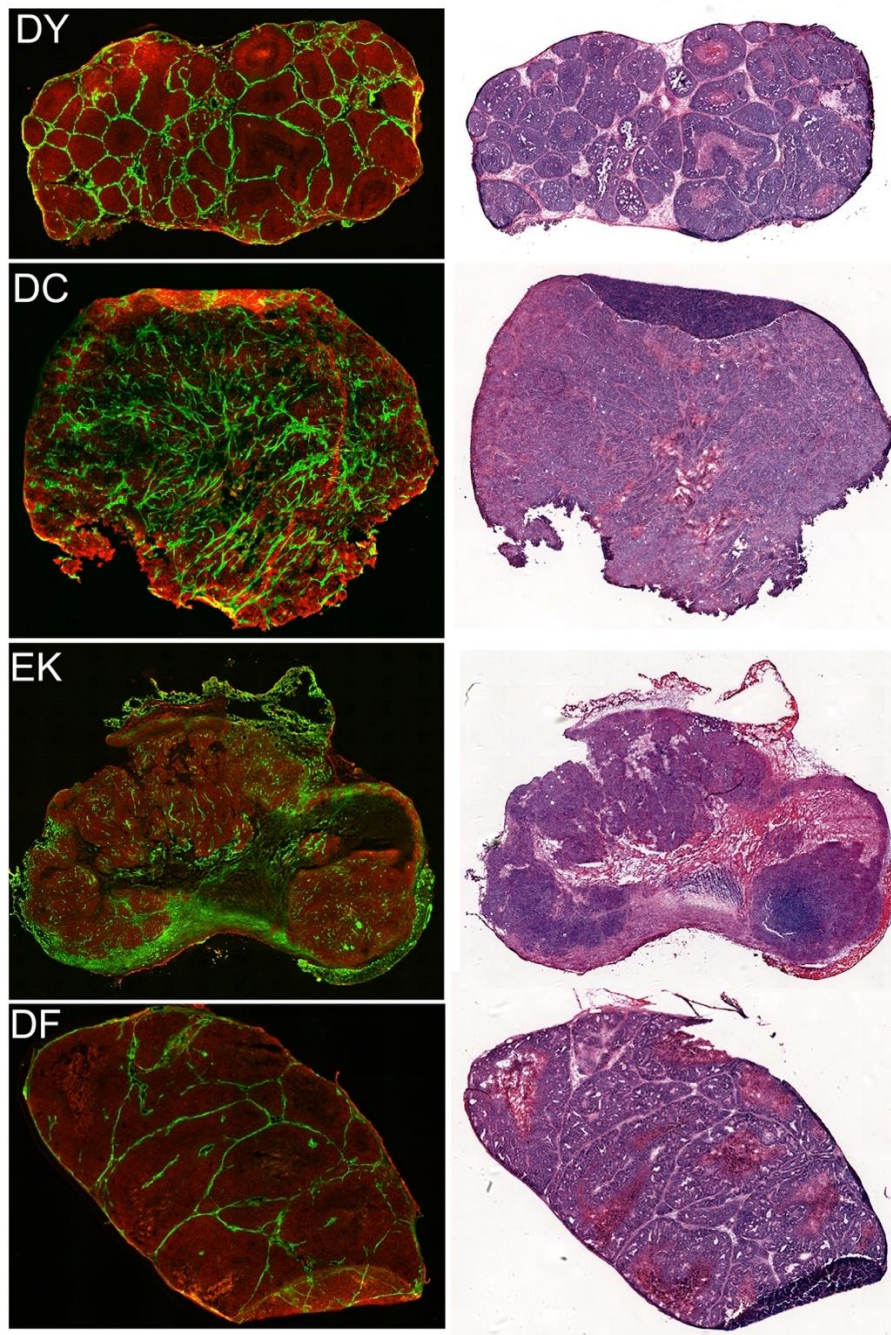




**Supplemental Fig. 9.** Serial PET imaging of  $^{89}\text{Zr}$ -DFO-AMG102 in PDX DF and EK bearing mice with unknown levels of HGF at 24, 48, 72, and 120 h p.i. ( $\sim 30 \mu\text{g}$ ,  $\sim 130\text{-}150 \mu\text{Ci}$ ,  $\sim 4.8\text{-}5.6 \text{ MBq}$ ,  $200 \mu\text{L}$  sterile saline), showing low uptake in tumors suggesting very low levels of HGF protein,  $\sim 5\text{-}10 \text{ \%ID/g}$ , EPR uptake only.

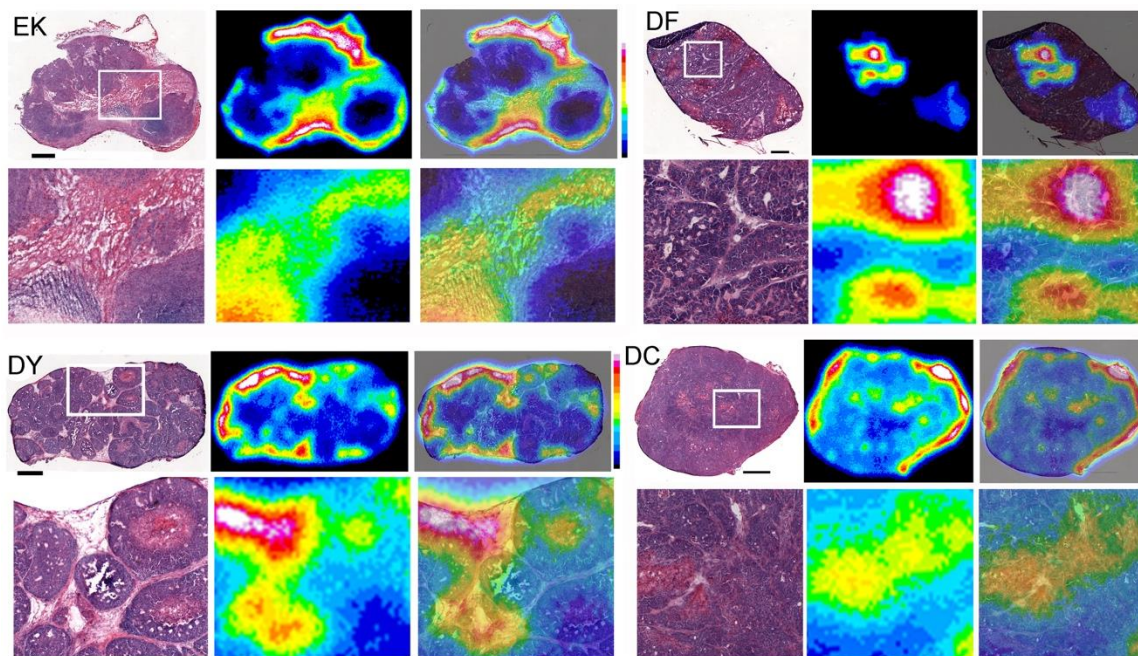


**Supplemental Fig. 10.** Autoradiography of  $^{89}\text{Zr}$ -DFO-AMG102 in patient-derived xenograft mouse models (subcutaneous), obtained at time of necropsy (120 h p.i.) after PET imaging, with all tumor sections run on the same phosphor-plate to obtain relative radiation intensity.



**Supplemental Fig. 11.** Autoradiography of  $^{89}\text{Zr}$ -DFO-AMG102 in patient-derived xenograft mouse models (subcutaneous), obtained at time of necropsy (120 h p.i.) after PET imaging, with the images displayed showing histology from hematoxylin and eosin staining (right), and immunofluorescence staining shown in green for perlecan (extracellular matrix/stroma) and red for anti-HGF antibody on the left, with all 4 tumors having very little HGF present (red color intensity not normalized for image acquisition time, meaning the gain has been artificially turned up to visualize the red color, and despite the intense red color there is very little HGF actually present, as confirmed by ELISA assay). HGF levels in these samples are similar to those observed in MKN45 shown in the manuscript Fig. 7.





**Supplemental Fig. 12.** Autoradiography of  $^{89}\text{Zr}$ -DFO-AMG102 in patient-derived xenograft mouse models (subcutaneous), obtained at time of necropsy (120 h p.i.) after PET imaging, with the images displayed showing histology from hematoxylin and eosin staining (left), autoradiography (middle), and an overlap of both (right).